Supplementary Information

Mapping the brain-wide network effects by optogenetic activation of the corpus callosum

Yi Chen[1,2], Filip Sobczak[1,2], Patricia Pais-Roldán[1,2], Cornelius Schwarz[3], Alan P. Koretsky[4], Xin Yu[1, 5*]

1 Research Group of Translational Neuroimaging and Neural Control, High-field Magnetic Resonance, Max Planck Institute for Biological Cybernetics, Tübingen, Baden-Württemberg, Germany

2 Graduate Training Centre of Neuroscience, University of Tübingen, Tübingen, Baden-Württemberg, Germany

3 Werner Reichardt Center for Integrative Neuroscience, Tübingen, Baden-Württemberg, Germany

4 National Institute of Neurological Disorders and Stroke, Bethesda, Maryland, United States of America

5 Athinoula A. Martinos Center for Biomedical Imaging, Massachusetts General Hospital and Harvard Medical School, Charlestown, Massachusetts, United States of America

Corresponding author:

Dr. Xin Yu

Email: xin.yu@tuebingen.mpg.de, xyu9@mgh.harvard.edu

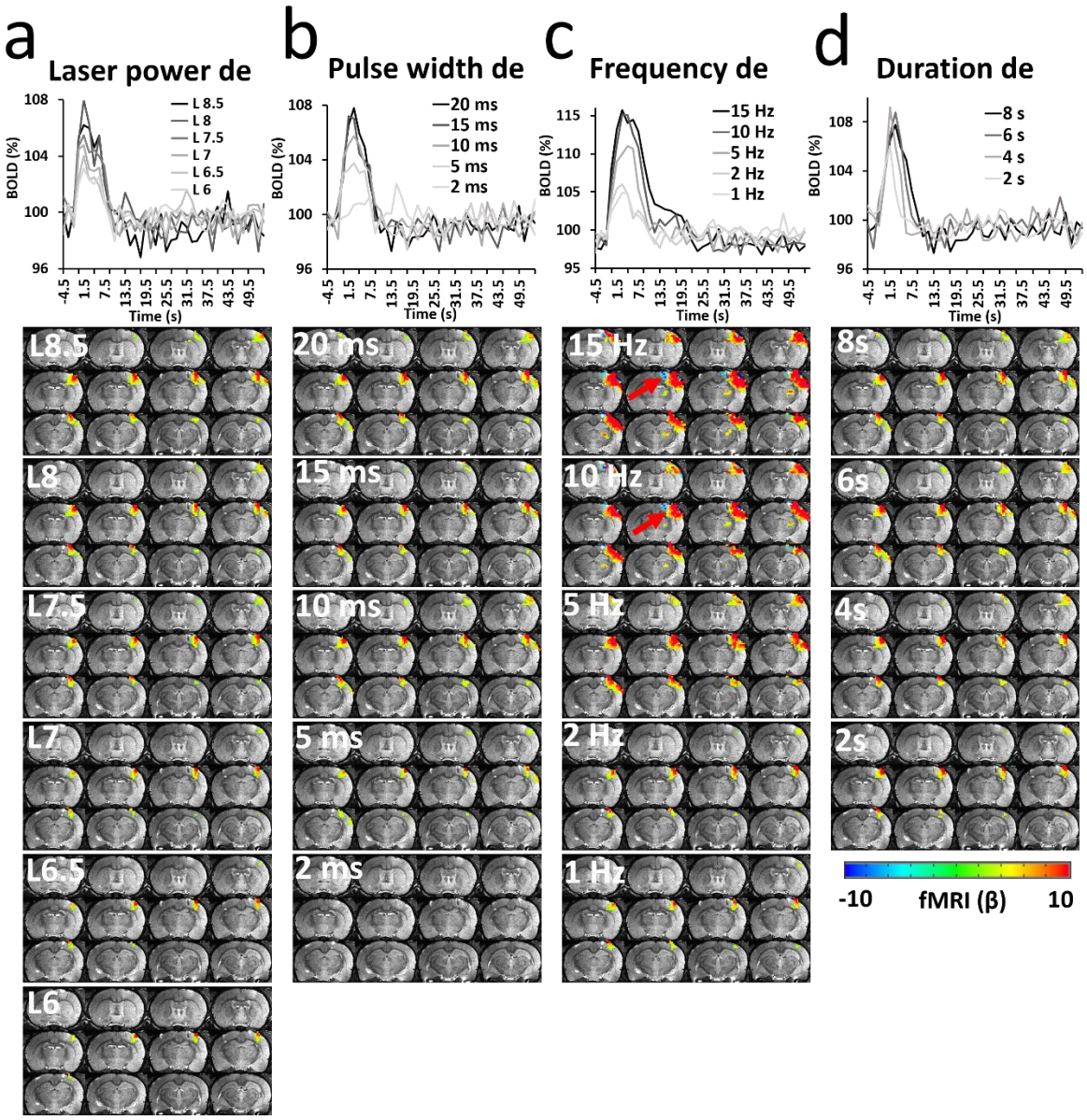

Supplementary Figure 1. Representative functional maps and time courses of the fMRI signal (average of 13 epochs, 60 s per epoch) upon CC light activation with (**a**) laser power dependency (2 Hz, 8 s, 20 ms pulse width), (**b**) pulse width dependency (2, 5, 10, 15 and 20 ms pulse width, 2 Hz, 8 s, L 8), (**c**) frequency dependency (1, 2, 5, 10 and 15 Hz, 8 s, L 8, 20 ms pulse width) and (**d**) duration dependency (2, 4, 6 and 8 s, 2 Hz, 20 ms pulse width, L 8). It is noteworthy that exposure to light with high frequency (10 and 15 Hz) at high power (35 mW) led to negative BOLD (due to off-resonance effect), inducing artifacts close to the fiber tip (red arrow), as well as very strong antidromic activity. GLM-based t-statistics in AFNI is used, p (corrected) < 0.005.

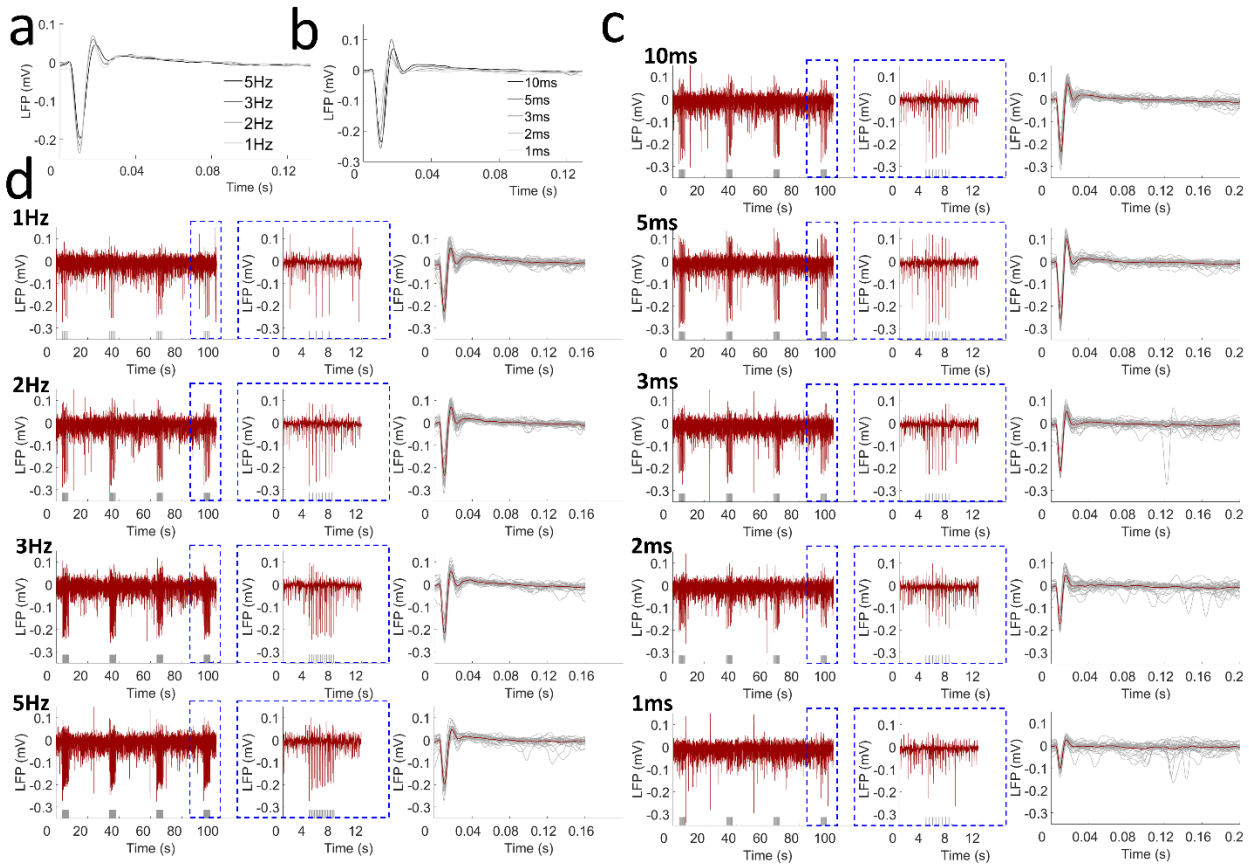

Supplementary Figure 2. The light-driven antidromic LFP with frequency and pulse width dependency of a representative rat. (**a**) Averaged LFP driven by light pulses at different frequencies (1, 2, 3 and 5 Hz; 10 ms pulse width, L 7.5, 4 s stimulation 26 s rest, 16 epochs). (**b**) Averaged LFP driven by light pulses at different pulse widths (1, 2, 3, 5 and 10 ms pulse width; 2 Hz, L 7.5, 4 s stimulation 26 s rest, 16 epochs). (**c**) The raw LFP trace by optogenetic stimulation (*left*, 4 epochs), the enlarged representative LFP for one epoch (*middle*) and the averaged LFP from one trial (red line).The grey lines show all the LFP from this trial (*right*) upon different stimulation frequencies. (**d**) The raw LFP trace during optogenetic stimulation (*left*, 4 epochs), the enlarged representative LFP for one epoch (*middle*) and the averaged LFP from one trial (red line). The grey lines show all the LFP from this trial (*right*) upon different stimulation light pulse widths. Grey lines beneath the LFP indicate the stimulation.

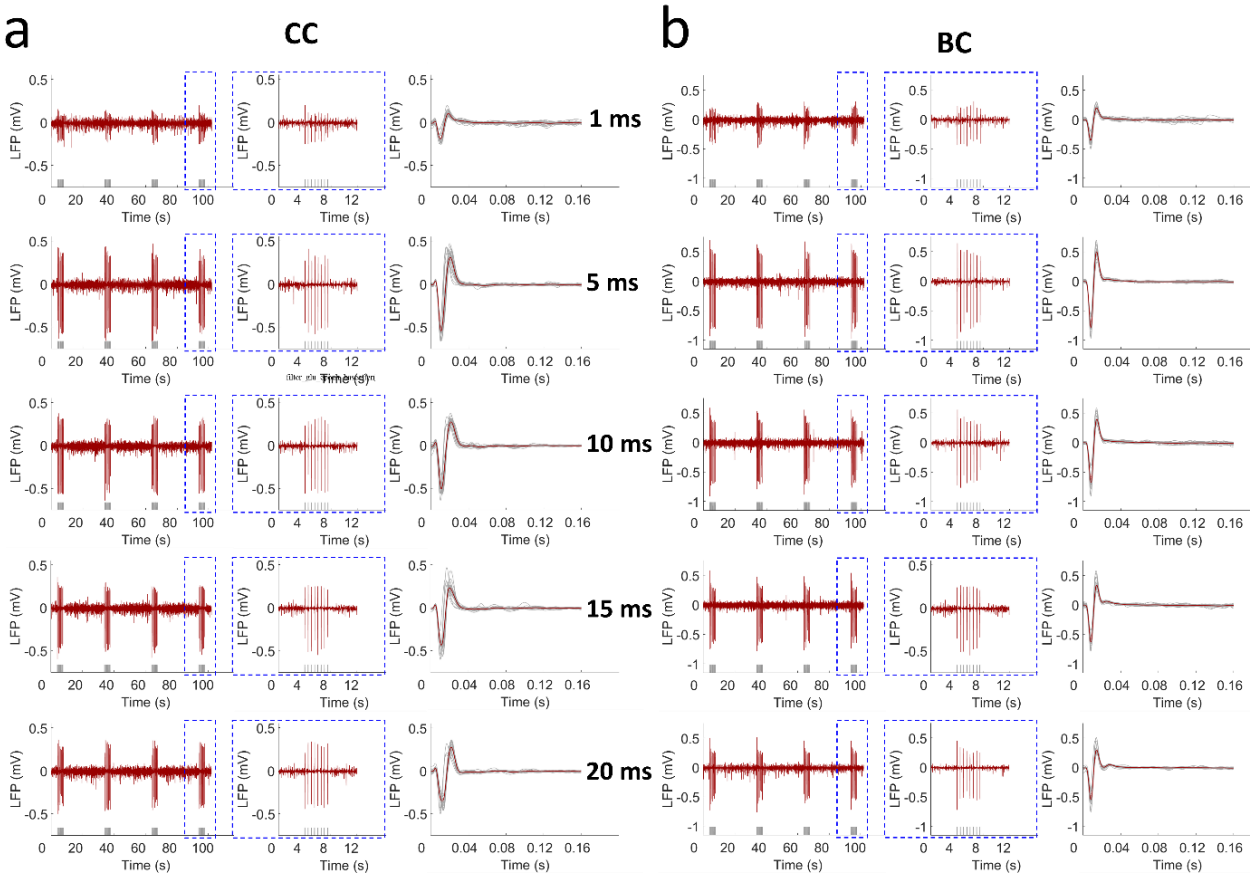

Supplementary Figure 3. Light-driven LFP for antidromic activity from CC (**a**) stimulation and BC (**b**) direct stimulation showing similiar pattern with pulse width dependency of a representative rat. Every panel in **a** and **b** shows the raw LFP trace observed upon optogenetic stimulation (*left*, 4 epochs), the enlarged representative LFP for one epoch (*middle*) from the dashed blue box and the averaged LFP from one trial (red line). The grey lines show all the LFP from this trial (*right*). Grey lines beneath the LFP indicate the stimulation.

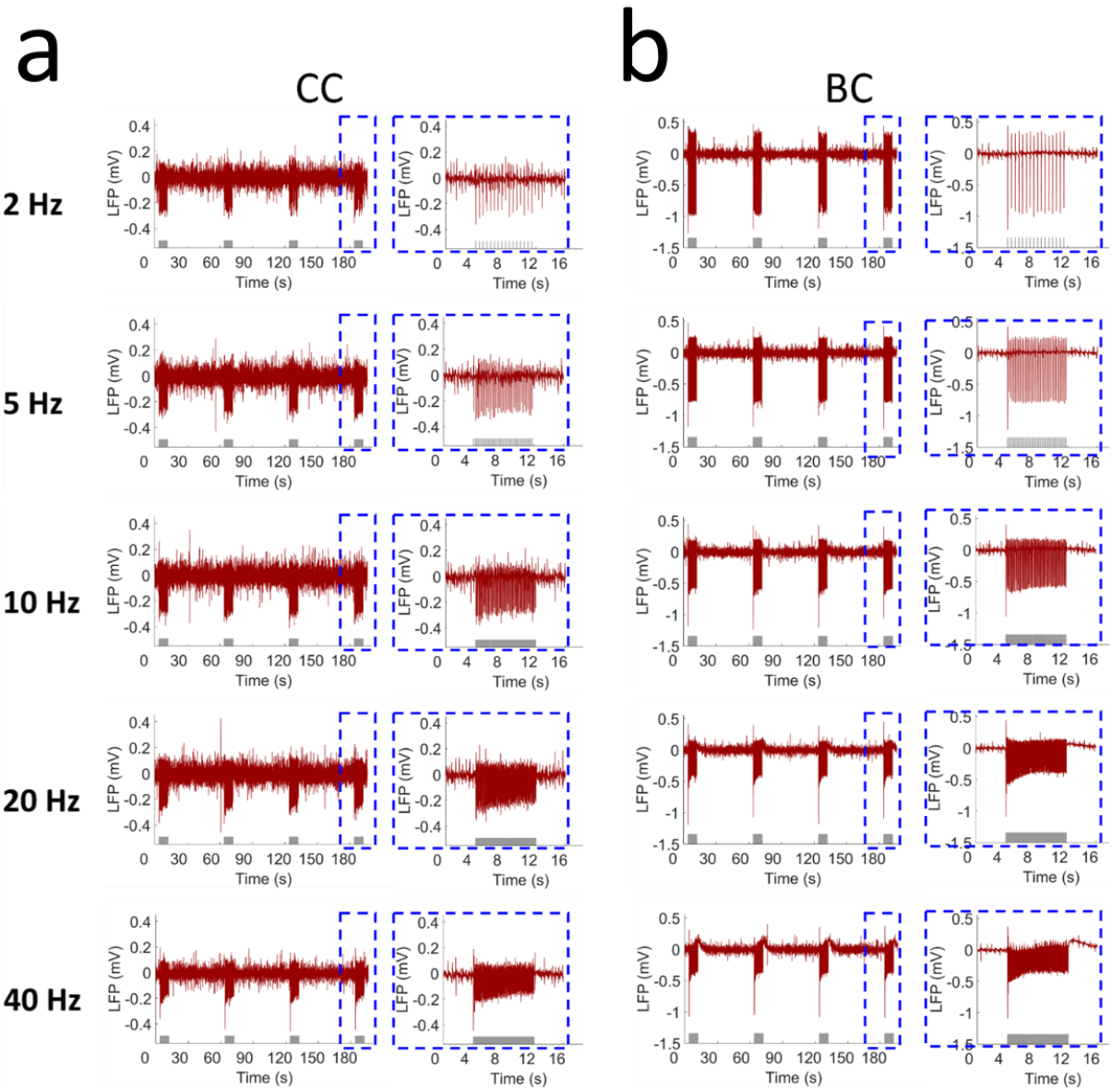

Supplementary Figure 4. Light-driven LFP for antidromic activity from CC stimulation (**a**) and BC direct stimulation (**b**) showing similar pattern with frequency dependency of a representative rat. Every panel in **a** and **b** shows the raw LFP trace by optogenetic stimulation (*left*, 4 epochs), the enlarged representative LFP for one epoch (*right*) from the dashed blue box. Grey lines beneath the LFP indicate the stimulation.

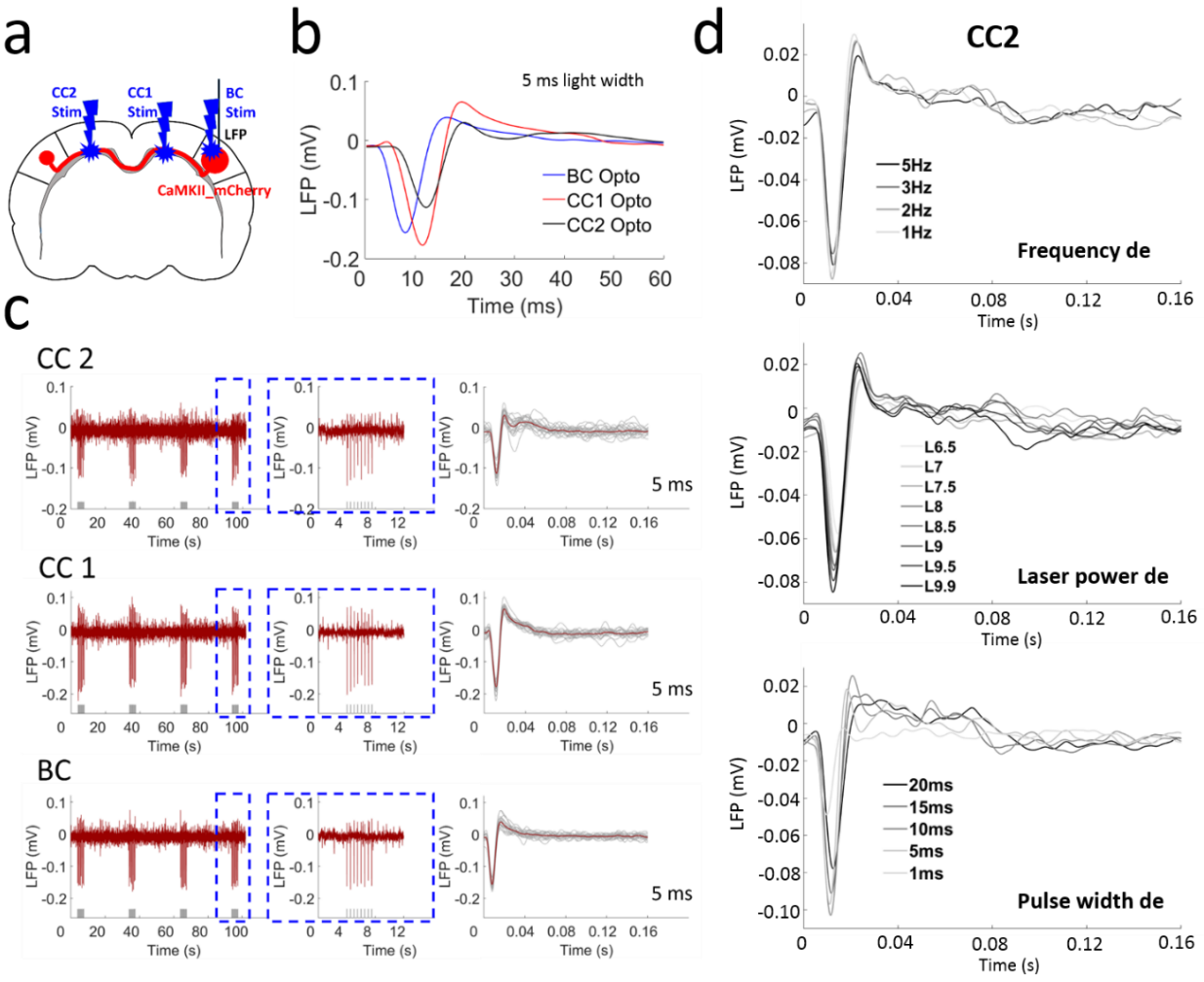

Supplementary Figure 5. Light-driven LFP for antidromic activity from CC stimulation in both hemispheres and BC direct stimulation. (**a**) The schematic plan for the experiment design. (**b**) Averaged LFP from the CC2 stimulation in the hemisphere opposite to the virus injection site (blue line), CC1 stimulation in the same hemisphere (red line) and BC direct stimulation (black line) shown different temporal features. (**c**) The raw LFP trace by optogenetic stimulation (*left*, 4 epochs), the enlarged representative LFP for one epoch (*middle*) from the dashed blue box and the averaged LFP from one trial (red line). The grey lines show all the LFP from this trial (*right*). (**d**) Averaged LFP upon optogenetic stimulation of CC2 with frequency (*upper panel*), laser power (*middle panel*) and pulse width (*lower panel*) dependency showing reliably detected antidromic activity.

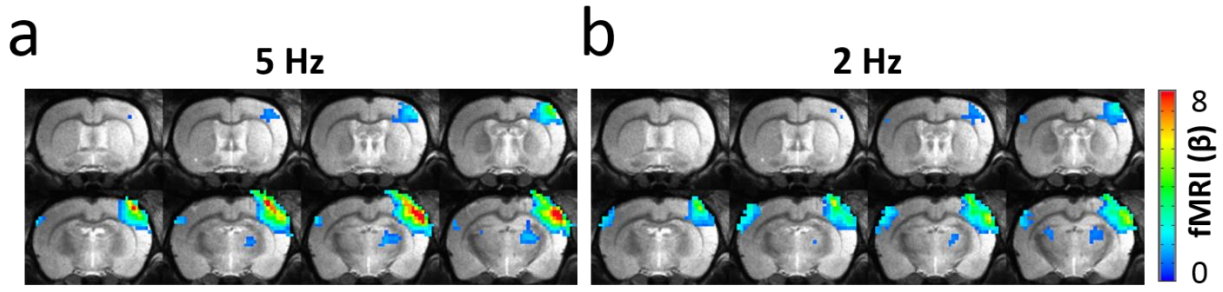

Supplementary Figure 6. Light-driven functional maps demonstrating opposite relationships for antidromic and orthodromic activities in the BC from 8 rats to 5 Hz (**a**) and 2 Hz (**b**). The antidromic activity in the right hemisphere and the orthodromic activity in the left hemisphere responses to 5 Hz was stronger and weaker, respectively, compared to 2 Hz. GLM-based t-statistics in AFNI is used. p (corrected) < 0.01.

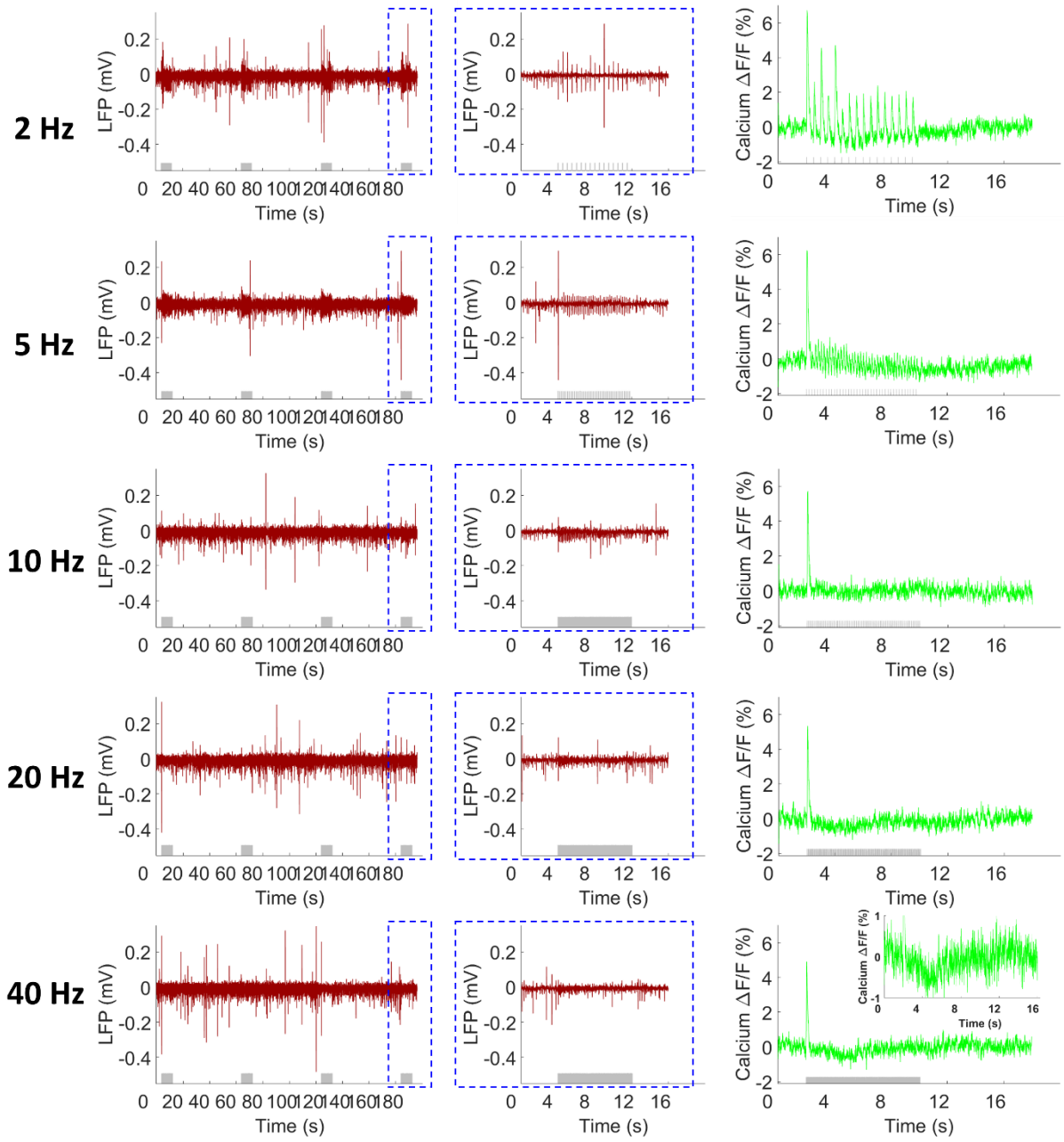

Supplementary Figure 7. The frequency dependency of simultaneous LFP (red) and calcium response signals (green) recorded at the left BC upon callosal optogenetic stimulation. Every panel shows the raw LFP trace elicited by optogenetic stimulation (*left*, 4 epochs), the enlarged representative LFP for one epoch from the dashed blue box (*middle*) and averaged calcium signal (8 s stimulation 52 s rest, 15 epochs, L9, pulse width 10 ms). Grey lines beneath the LFP and calcium signals indicate the stimulation. The enlarged figure on the bottom right panel shows the baseline deflection for the 40 Hz stimulation.

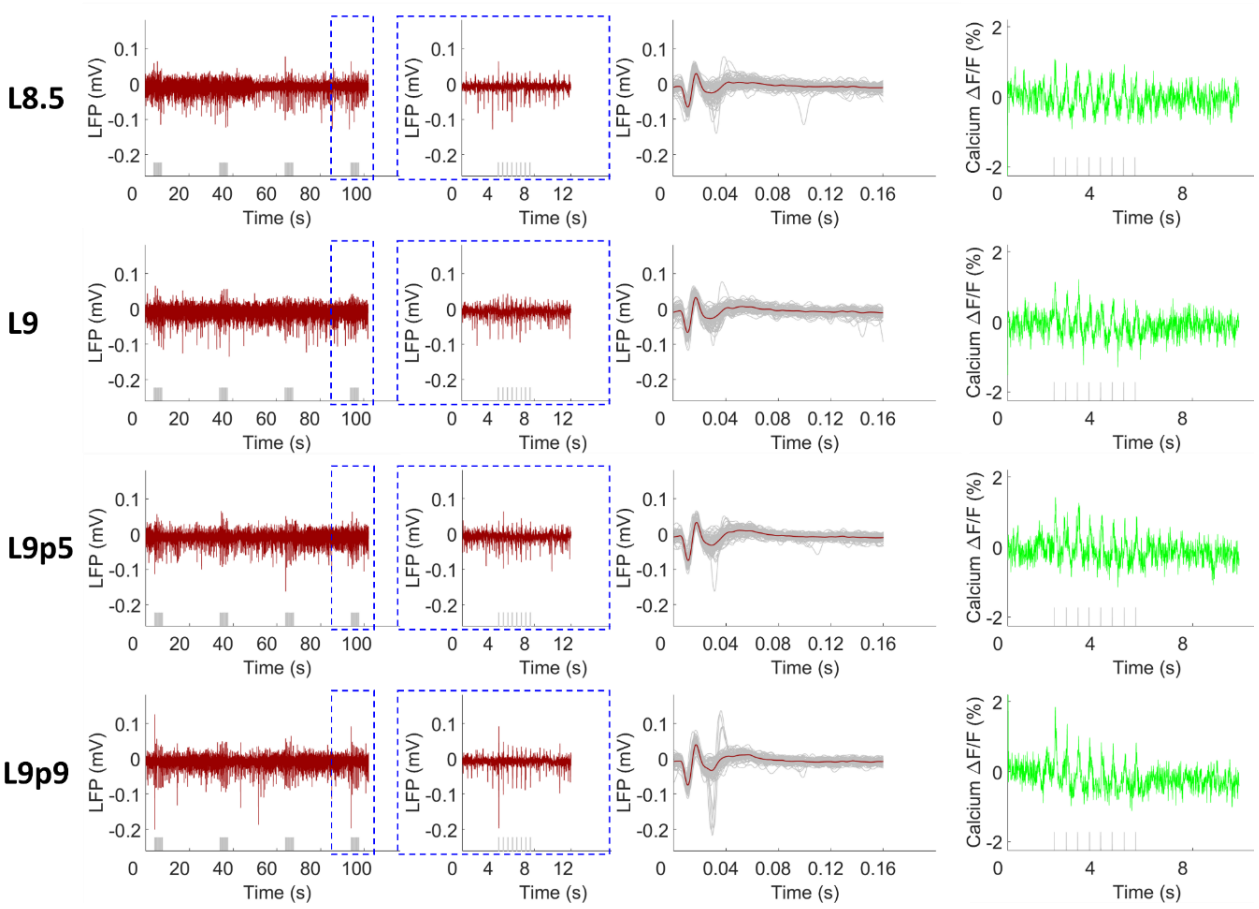

Supplementary Figure 8. The laser power dependency of simultaneous LFP (red) and calcium signals (green) showing that both amplitudes increased as a function of the laser power (detailed laser power in Methods). Every panel shows the raw LFP trace elicited by optogenetic stimulation (*left*, 4 epochs), the enlarged representative LFP for one epoch from the dashed blue box (*middle*), the averaged LFP from one trial (red line). Grey lines showing all the LFP from this trial (*right*) and the averaged calcium signal (4 s stimulation 26 s rest, 11 epochs, 2 Hz, pulse width 10 ms). Grey lines beneath the LFP and calcium signals indicate the stimulation.

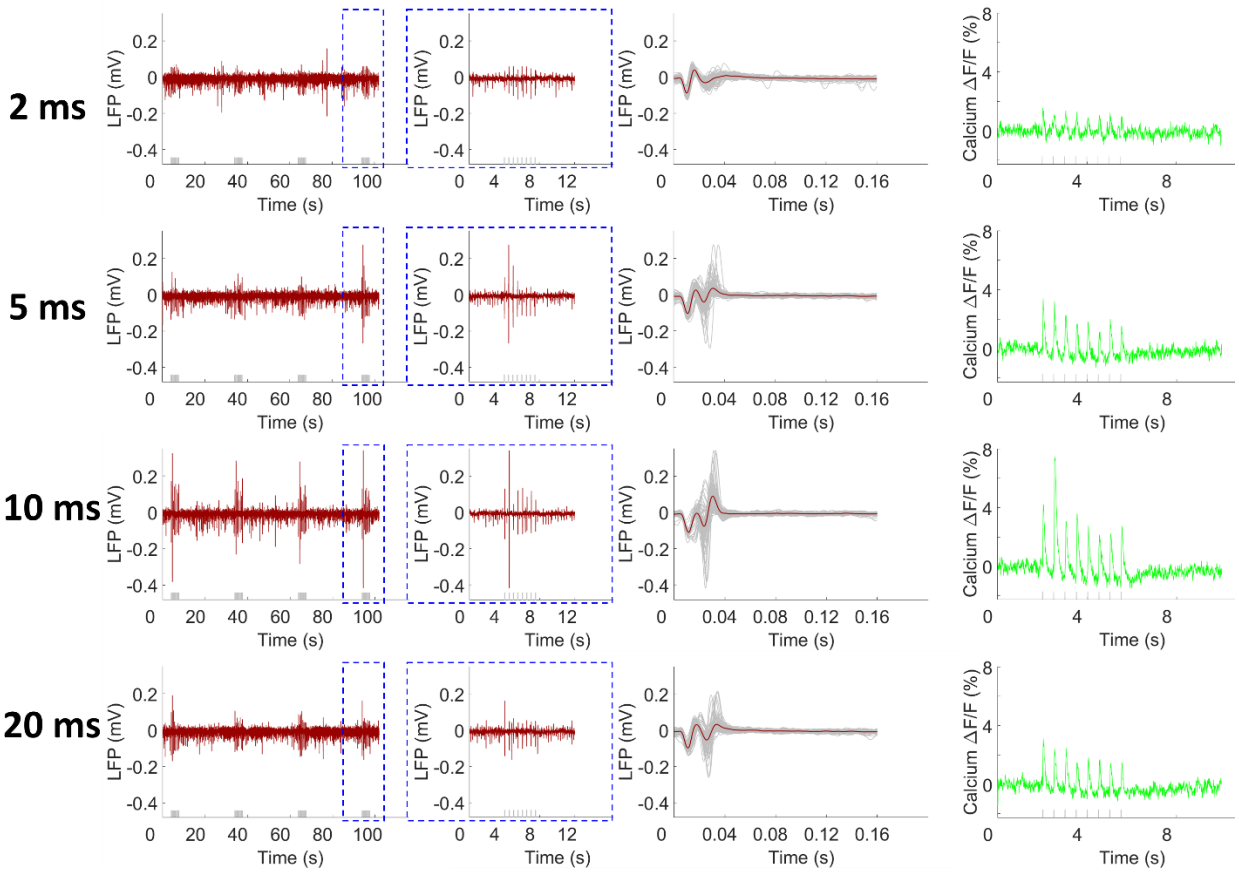

Supplementary Figure 9. The laser pulse width dependency of simultaneous LFP (red) and calcium signals (green). Calcium signals increased and the LFP pattern demonstrated stronger depolarization according to the increased pulse width at 2 ms, 5 ms and 10 ms. In contrast, for the 20 ms pulse width stimulation, there was decreased calcium signal and weaker depolarization of LFP. Every panel shows the raw LFP trace elicited by optogenetic stimulation (*left*, 4 epochs), the enlarged representative LFP for one epoch from the dashed blue box (*middle*), the averaged LFP from one trial (red line, with the grey lines showing all the LFP from this trial) (*right*) and the averaged calcium signal (2 Hz, 4 s stimulation 26 s rest, 11 epochs, L9). Grey lines beneath the LFP and calcium signals indicate the stimulation.

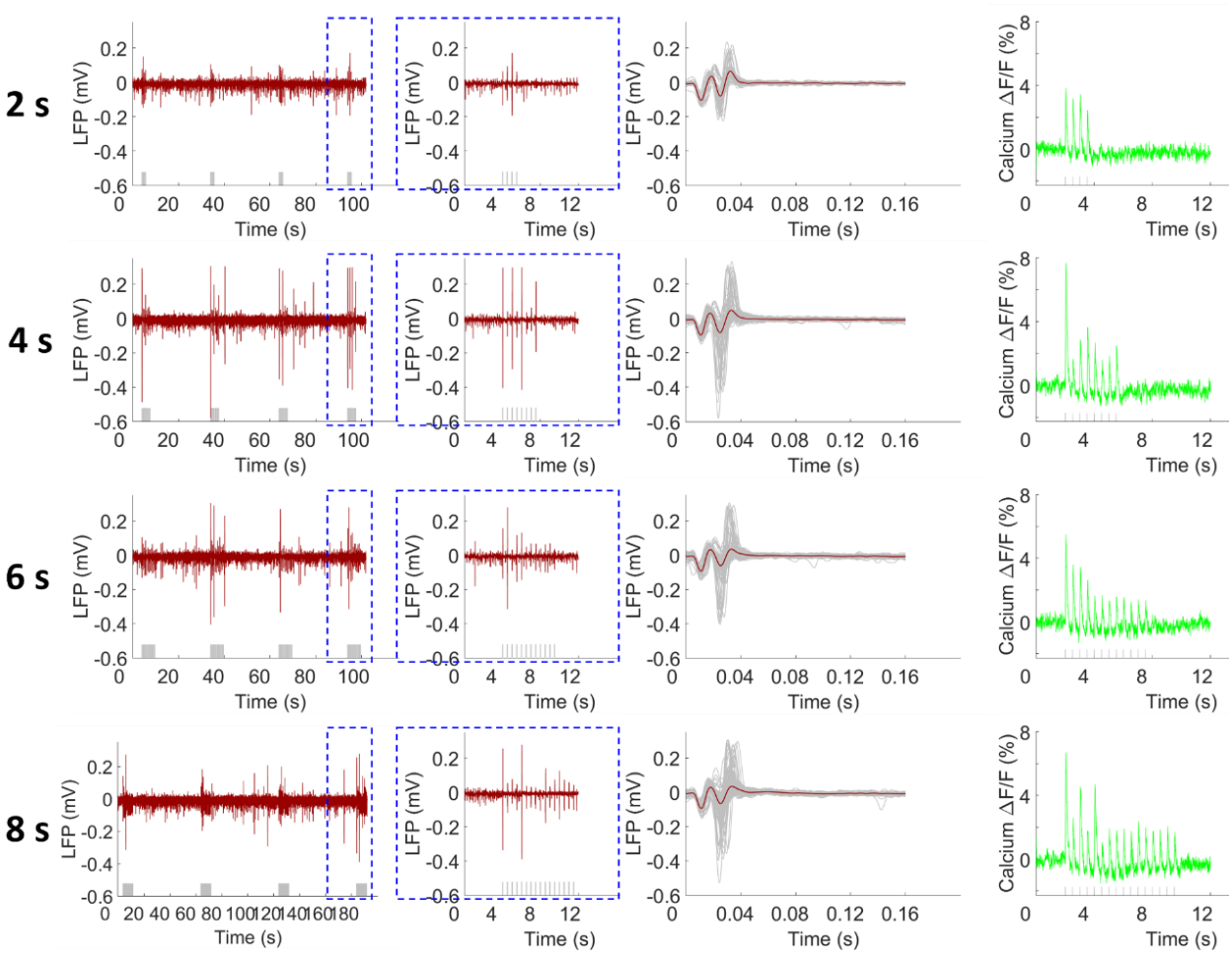

Supplementary Figure 10. The duration dependency of simultaneous LFP (red) and calcium signals (green). Every panel shows the raw LFP trace elicited by optogenetic stimulation (*left*, 4 epochs), the enlarged representative LFP for one epoch from the dashed blue box (*middle*), the averaged LFP from one trial (red line, with the grey lines showing all the LFP from this trial) (*right*) and the averaged calcium signal (2 Hz, 11 epochs, L9, pulse width 10 ms). Grey lines beneath the LFP and calcium signals indicate the stimulation.

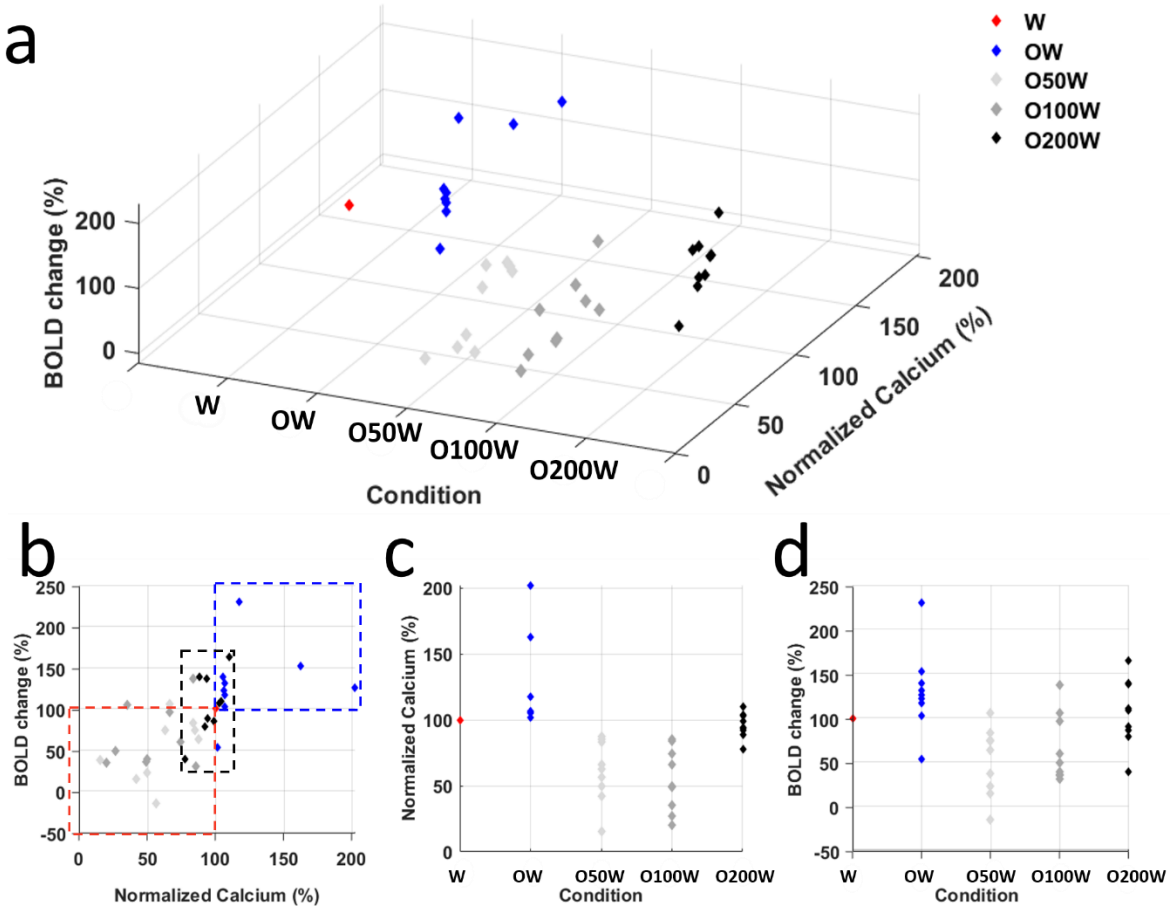

Supplementary Figure 11. The scatter plots of the evoked BOLD and calcium signals for 5 stimulation conditions (W, OW, O50W, O100W and O200W) in 9 animals. (**a**) 3D plot of the BOLD changes (Z axis), calcium changes (Y axis) and stimulation conditions (X axis). Both BOLD and calcium signals are normalized to condition W. (**b**) View from the correlation of BOLD changes with calcium signals. The central red diamond is the baseline to which the data were normalized. Blue diamonds represent the condition OW, most of them distributed in the dashed blue box, showing increased neuronal activities. Light grey diamonds and dark grey diamonds represent the condition O50W and O100W, respectively, most of them located in the dashed red box, showing suppressed neuronal activities. (**c**) Normalized calcium signals as a function of condition. (**d**) Normalized BOLD changes as a function of condition. W: whisker stimulation only, OW: simultaneous optical and whisker stimulation, O[x]W optical stimulation followed by [x] ms-delayed whisker stimulation.

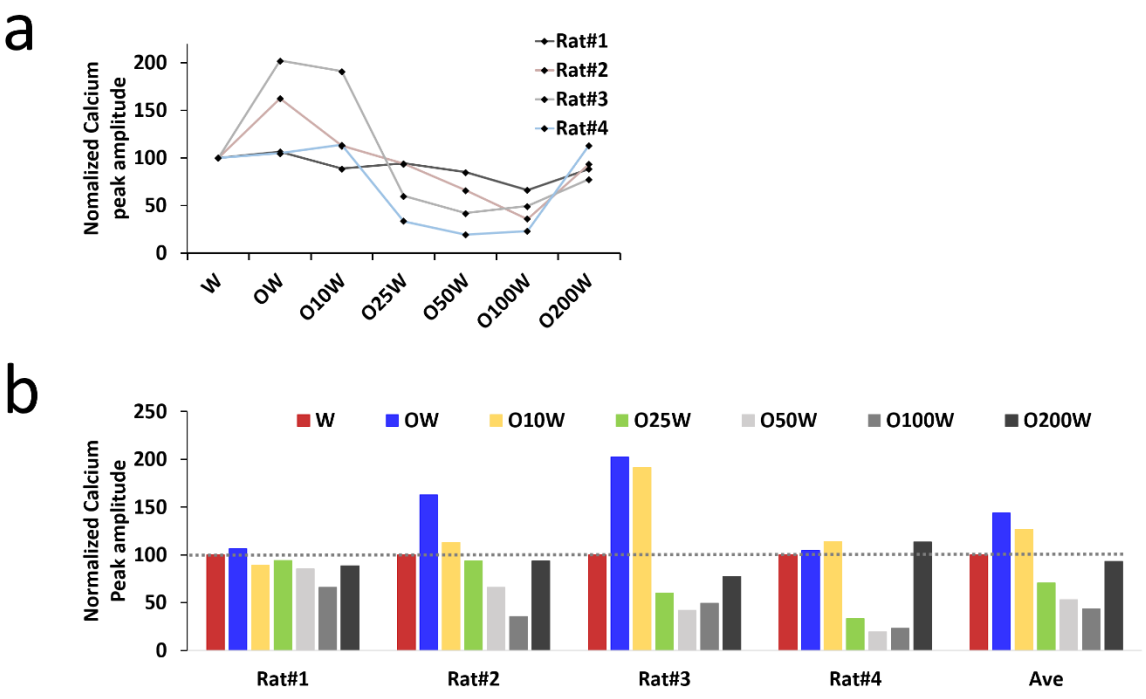

Supplementary Figure 12. The effect of conditioning stimuli in the sensory evoked calcium signals in the left hemisphere for 7 refined conditions (W, OW, O10W, O25W, O50W, O100W and O200W). (**a**) The scatter plot of the calcium signals normalized to condition W from 4 rats. (**b**) The individual pattern changes of calcium signals from 4 animals, as well as the averaged calcium signal change pattern for all the 7 conditions.

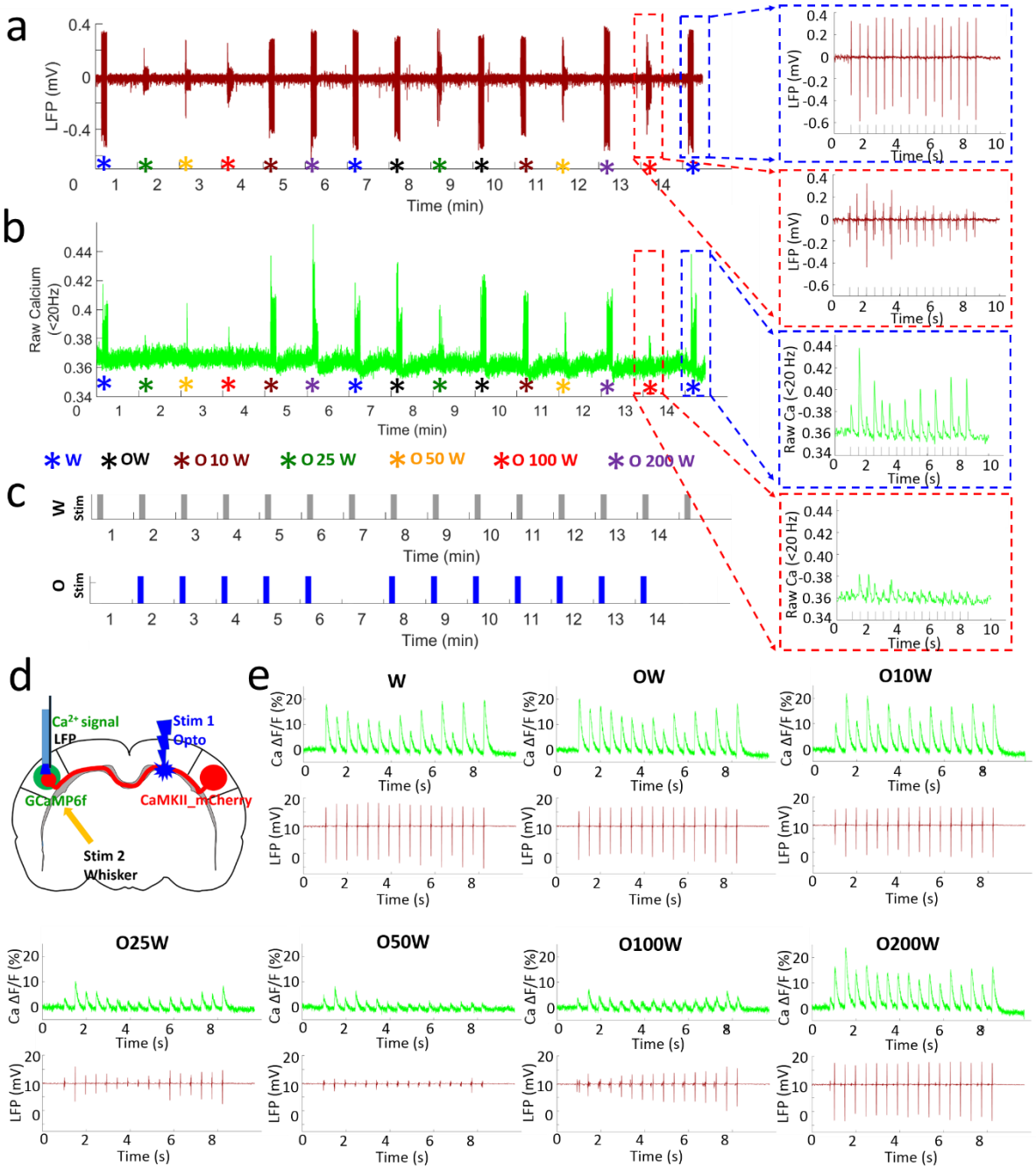

Supplementary Figure 13. Typical LFP (red) and calcium signals (green) of one trial from a representative rat. (**a**) Different amplitudes of LFP and (**b**) calcium signal changes showing the different neuronal activity upon seven randomized stimulation conditions. (**c**). Simplified diagram representing the typical calcium signals and LFP for condition W (blue dash boxes in **a** and **b**, upper graph in **c**) and O100W (red dash boxes in **a** and **b**, lower graph in **c**) in one epoch. (**d**) Schematic of the experimental design. (**e**) Averaged calcium signals and LFP in left barrel cortex, further confirming the spatial and temporal features of sensory-evoked cortical activity pattern shaped by callosal inputs. W: whisker stimulation only, OW: simultaneous optical and whisker stimulation, O[x]W optical stimulation followed by [x] ms-delayed whisker stimulation.

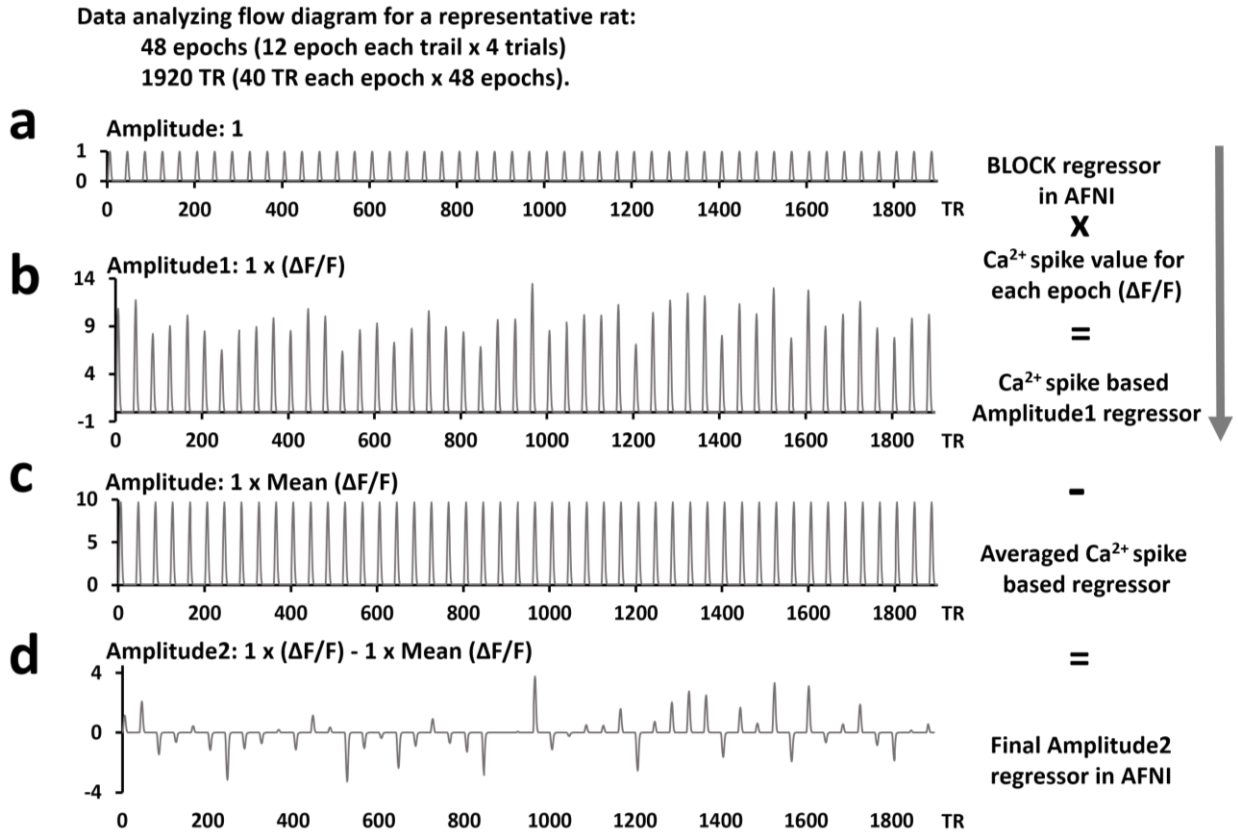

Supplementary Figure 14. The flow diagram to generate the calcium signal-based regressor for the fMRI correlation map. (**a**) version 1 of the regressor, generated with the parameter BLOCK (L, 1), which generates a convolution of a square wave of duration L with the stimulation train and makes a peak amplitude of block response = 1. (**b**) the variable calcium amplitude of each epoch from a representative rat is used to generate the AM1 (amplitude modulated 1) regressor in 3dDeconvolve command in AFNI. (**c**) the averaged calcium amplitude of all the epochs is used to generate the regressor of no interest. (**d**) by computing '**b** – **c**', the differences from the mean calcium amplitude can be detected. This new vector constitutes the final regressorAM2. 'AM2' allows to detect voxels that activate but do not change proportionally to the amplitude factor, as well as provides a direct measure of the proportionality of the activation in response to changes in the input amplitude factors (from the description of 3dDeconvolve program in AFNI).

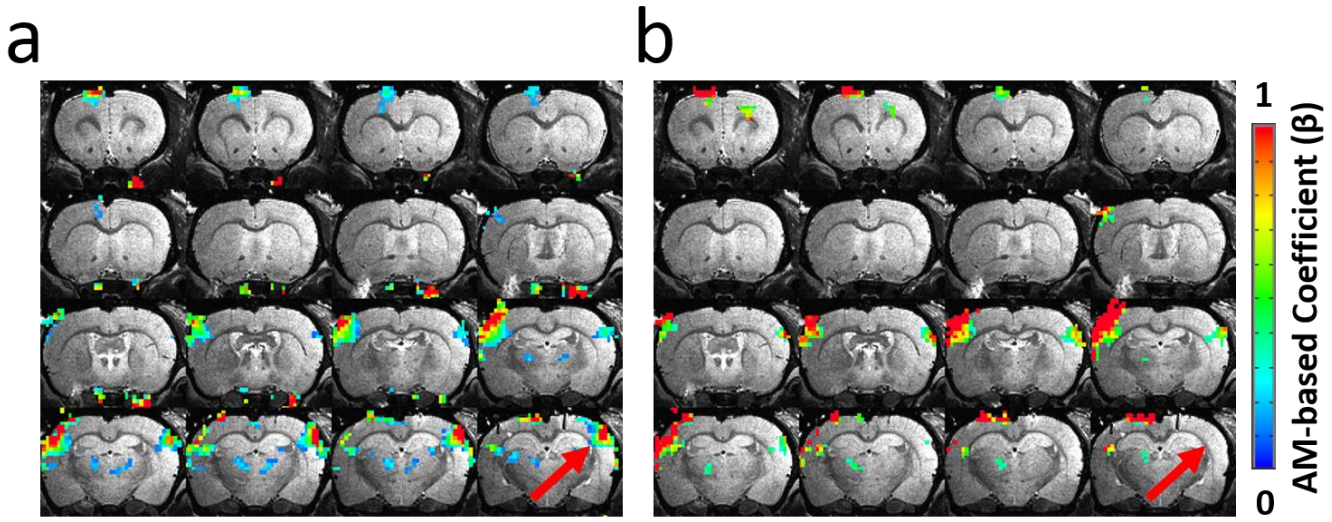

Supplementary Figure 15. AM1 and AM2-based correlation analysis. Red arrow in **a** (AM1) shows strong correlation for the antidromic activity, while not in **b** (AM2).